Kobe University Repository : Kernel

PDF issue: 2025-12-05

Endothelial cell-selective adhesion molecule modulates atherosclerosis through plaque angiogenesis and monocyte-endothelial interaction

Inoue, Michihiko ; Ishida, Tatsuro ; Yasuda, Tomoyuki ; Toh, Ryuji ; Hara, Tetsuya ; Husni M. Cangara ; Rikitake, Yoshiyuki ; Taira, Kazuki…

(Citation)
Microvascular research,80(2):179-187

(Issue Date)
2010-09

(Resource Type)
journal article

(Version)
Accepted Manuscript

(URL)
https://hdl.handle.net/20.500.14094/90001480

Endothelial cell-selective adhesion molecule modulates atherosclerosis through plaque angiogenesis and monocyte-endothelial interaction

Michihiko Inoue[1], Tatsuro Ishida[1], Tomoyuki Yasuda[1], Ryuji Toh[1],

Tetsuya Hara[1], Husni M. Cangara[1], Yoshiyuki Rikitake[1], Kazuki Taira[1],

Li Sun[1], Ramendra K Kundu[2], Thomas Quertermous[2], Ken-ichi Hirata[1]

[1]Division of Cardiovascular Medicine, Kobe University Graduate School of Medicine;

[2]Division of and Cardiovascular Medicine, Stanford University School of Medicine.

Short title: ESAM deficiency attenuates atherosclerosis

Address for correspondence: Tatsuro Ishida, MD, PhD.

Division of Cardiovascular Medicine, Kobe University Graduate School of Medicine,

7-5-1 Kusunoki-cho, Chuo-ku, Kobe 650-0017, Japan.

Phone: +81-78-382-5846, Fax: +81-78-382-5859, E-mail: ishida@med.kobe-u.ac.jp

Abstract

Endothelial cell-selective adhesion molecule (ESAM) is a new member of the immunoglobulin superfamily, which is expressed in vascular endothelial cells. Previous studies have demonstrated that ESAM regulates angiogenesis, endothelial permeability, and leukocyte transmigration. However, little is known concerning the role of ESAM in atherosclerosis. In this study, we assessed the effects of *ESAM* inactivation on atherosclerosis in mice. *ESAM*-/- mice were bred with *apoE*-/- mice to generate double knockout mice, and the aortic lesion size of *apoE*-/- and *ESAM*-/-*apoE*-/- mice was compared histologically. Although plasma cholesterol levels were higher in *ESAM*-/-*apoE*-/- mice, the lesion size was markedly smaller than in *apoE*-/- mice. *ESAM*-/-*apoE*-/- mice exhibited a decrease in the number of vasa vasorum and macrophages in the vessel wall. *In vitro* adhesion assays showed that THP-1 cells, which did not express ESAM, bound to the ESAM-coated culture plates, suggesting that ESAM may interact with heterophilic ligand(s) on monocytes. Moreover, downregulation of *ESAM* by siRNA in the endothelial monolayer diminished transendothelial migration of THP-1 cells. In conclusion, *ESAM* inactivation can reduce susceptibility to atherosclerosis by inhibiting plaque neovascularization and macrophage infiltration into the atheroma.

Key words: atherosclerosis, adhesion molecule, endothelium, vasa vasorum, angiogenesis, monocyte, macrophage.

1. Introduction

Atherosclerosis is a complex process characterized by accumulation of lipids and fibrous elements in the large arteries. The vascular endothelium is known to protect the vessel wall against the development of atherosclerosis because it inhibits adhesion of circulating inflammatory cells to the vessel wall, vascular smooth muscle cell migration and proliferation, and thrombus formation. Endothelial dysfunction therefore directly contributes to the initiation and progression of atherosclerosis.(Price and Loscalzo, 1999; Sprague and Khalil, 2009; Springer, 1990; Taddei et al., 2003) Infiltration of inflammatory cells into the vessel wall is a crucial step in the development of atherosclerosis, especially since the early lesions of atherosclerosis involve the accumulation of cholesterol-engorged macrophages. The vascular endothelium thus plays a pivotal role in the process of atherosclerosis including macrophage recruitment.(Ley et al., 2007) Endothelial cells feature several adhesion molecules at the cell surface such as vascular cell adhesion molecule-1 (VCAM-1), intercellular adhesion molecule-1 (ICAM-1), and platelet selectin (P-selectin).(Cybulsky et al., 2001) These molecules are upregulated by atherogenic stimuli and thereby contribute to the adhesion and infiltration of macrophages. In this context, atherosclerosis is considered as an inflammatory disease. (Ross, 1999)

In addition, it has been postulated that progression of atherosclerosis depends on new blood vessel formation, which is referred to as vasa vasorum, in the vessel wall. The function of vasa vasorum is to deliver nutrients and oxygen to vessel walls and to remove waste products, either produced by cells in the wall or introduced by diffusional transport through the endothelium. (Bolla et al., 1999; Ritman and Lerman, 2007) Previous studies have demonstrated that increases in the volume of vasa vasorum match those in the needs of the

growing vessel wall.(Moulton et al., 2003) In fact, inhibition of microangiogenesis by angiostatin can interrupt the secondary reduction of macrophage accumulation, which established that vasa vasorum could be the source of the inflammatory cells.(Moulton et al., 2003) In addition, recombinant plasminogen activator inhibitor (rPAI-1_{23}), which has significant antiangiogenic activity, inhibits growth of vasa vasorum as well as vessels within the adjacent plaque and vessel wall through inhibition of fibroblast growth factor-2, which in turn leads to a reduction in plaque growth in atherogenic mouse.(Drinane et al., 2009) From these findings, it is reasonable to hypothesize that vasa vasorum may contribute to the formation of atherosclerosis through modulating infiltration of inflammatory cells and blood vessel formation in the plaque.

The endothelial cell-selective adhesion molecule (ESAM) is a new member of the immunoglobulin superfamily, which is highly expressed by vascular endothelial cells.(Hirata et al., 2001; Nasdala et al., 2002) ESAM has been shown to mediate homophilic and calcium-independent adhesion of endothelial cells.(Hirata et al., 2001) Previous studies have demonstrated that ESAM regulates tumor angiogenesis, vascular permeability, and leukocyte transmigration both *in vitro* and *in vivo*.(Hara et al., 2009; Ishida et al., 2003; Wegmann et al., 2006) While these lines of evidence suggest that ESAM may play a pivotal role in the genesis of atherosclerosis, the role of ESAM in atherogenesis has not been reported. The *apolipoprotein E*-deficient (*apoE*-/-) mice has been extensively characterized in terms of the altered lipoprotein profiles and predisposition to atherosclerosis. *ApoE*-/- mice have markedly elevated serum cholesterol associated with increased VLDL/LDL-cholesterol and reduced HDL-cholesterol. As a result of this highly atherogenic lipoprotein profile, *apoE*-/- mice spontaneously develop complex atherosclerotic lesions. The aim of the study reported

here, was therefore to explore the role of ESAM in the murine model of atherosclerosis using *ESAM*-deficient (*ESAM*-/-) mice. To initiate studies investigating ESAM involvement in atherosclerosis, *ESAM*-/- mice with a C57Bl/6 background were bred with *apoE*-/- mice with a C57Bl/6 background. We tested how targeted inactivation of *ESAM* modulates formation and progression of the atherosclerotic plaque in *apoE*-/- mice through plaque angiogenesis and leukocyte-endothelium interaction.

2. Materials and Methods

2.1 Animal preparation

Homozygous *apoE-/-* mice with C57BL/6J background were obtained from the Jackson Laboratory (Bar Harbor, ME), and bred with *ESAM-/-* mice with a C57BL/6J background (Ishida et al., 2003) to generate *ESAM-/-apoE-/-* double knockout mice. Genotyping of the *apoE* locus was performed as described elsewhere.(Bolla et al., 1999) Genotyping of the *ESAM* locus was performed by means of polymerase chain reaction (PCR) using the following primers: 5'-ggcagctagaacactcttggggagg-3' (forward primer corresponding to the first intron in the *ESAM* genomic sequence), 5'-ggggagacttagaaccctaccgagc-3' (reverse primer corresponding to the first intron in *ESAM*), 5'-gtggatgtggaatgtgtgcgaggcc-3' (forward primer corresponding to the PGK promoter in the pKO Scrambler NTKV1901 targeting vector). The PCR was performed with 40 cycles at 93 ºC for 1 min, 54 ºC for 2 min, and 72 ºC for 2 min, and yielded a 330-bp in single band *ESAM-/-* mice, a 392-bp single band in *ESAM+/+* mice, and 330- and 392-bp double bands in *ESAM+/-* mice. *ApoE-/-* and *ESAM-/-apoE-/-* mice were weaned at 4 weeks of age and maintained on a normal chow diet (Oriental Yeast, Inc., Tokyo, Japan) for 12 weeks. Between 14 and 16 mice were included in each experimental subgroup. All animal

experiments were conducted according to the Guidelines for Animal Experiments of Kobe University Graduate School of Medicine and the Guide for the Care and Use of Laboratory Animals published by the National Institute of Health (NIH Publication No. 85-26, revised 1996).

2.2 Analysis of plasma lipids

Following an overnight fast, whole blood was collected by cardiac puncture into tubes containing 0.3 mg EDTA. Plasma was obtained by centrifugation at 8000 x g for 5 min at 4 °C. Plasma levels of total cholesterol (T-cho), high-density lipoprotein cholesterol (HDL-C), and triglyceride were measured with biochemial assays at Oriental Yeast, Inc.

2.3 Histological analysis of atherosclerotic lesions

The *apoE-/-* and *ESAM-/-apoE-/-* mice were euthanized at the age of 16 or 20 weeks (12 or 16 weeks on the chow diet), and the atherosclerotic lesions were analyzed as described previously.(Ishida et al., 2003; Ozaki et al., 2002; Pan et al., 2004; Sun et al., 2009) The ascending aortic samples were fixed in 10% buffered formalin phosphate, embedded in OCT compound and sectioned (10-μm thickness). Five consecutive sections, spanning 550 μm of the aortic root, were collected from each mouse and stained with hematoxylin and eosin (H&E), Sudan III, oil-red-O, Elastica van Gieson, or Masson's trichrome. For quantitative analysis of atherosclerosis, the total lesion area of the five sections was measured with the ImageJ software version 1.41 (National Institutes of Health, Bethesda, MD) as reported previously.(Ozaki et al., 2002) The amount of aortic lesion formation was measured as the percentage of lesion area per total area of the aorta.

En face analysis of the aortic lesion was performed as described previously.(Drinane et al., 2009; Ozaki et al., 2002) The distal part of the excised aorta (from aortic arch to iliac bifurcation) was dissected free from surrounding tissues, opened longitudinally, and pinned onto a silicon-coated dish. Oil-red-O stained aortas were subjected to image analysis with the ImageJ software.

2.4 Immunohistochemistry

Aortic sections of 8-12 μm were cut on a freezing microtome, and mounted on slides. After reduction of endogenous peroxidase activity with 0.1% hydrogen peroxide for 15 minutes at room temperature, nonspecific binding was blocked with 2% bovine serum albumin in PBS for 30 minutes. The tissue sections were then incubated for 24h with an anti-mouse monocyte/macrophage antibody (MOMA-2; Biosource International, Camarillo, CA) diluted in PBS, followed by incubation with N-Histofine® Simple Stain Mouse MAX PO (Nichirei Bioscience, Tokyo, Japan). For fluorescent analysis of vascular structures, aortic sections were incubated with Alexa Fluor568-conjugated anti-isolectin antibody (Invitrogen) or an FITC-conjugated anti-smooth muscle α-actin antibody (α-SMA; Sigma-Aldrich, St. Louis, MO). Samples were observed with the Biozero BZ-8000 fluorescent microscope (Keyence, Osaka, Japan).

Whole-mount analysis of vasa vasorum in the aorta was performed as previously described.(Drinane et al., 2009) Descending aortas were collected with a wide margin and made permeable in an overnight incubation at 4 ºC in PBS containing 0.5% Triton-X. The aortas were then incubated overnight at 4 ºC with 5 μg/mL Alexa Fluor568-conjugated anti-isolectin antibody in Can Get Signal immunostain solution. Isolectin-probed adventitial

vessels were imaged on a Zeiss LSM-510 META point scanning confocal microscope (Carl Zeiss Vision GmbH, Hallbergmoos, Germany),followed by the collection of Z stacks.

2.5 Cell culture, transfection, and siRNA experiment

Human umbilical vein endothelial cells (HUVEC), human aortic endothelial cells (HAEC), J774.1 cells (a murine monocyte cell line), and THP-1 (a human monocyte/macrophage cell line) were purchased from American Type Culture Collection (Manassas, VA). HUVEC at passages 4-10 was cultured on gelatin-coated culture plates according to the manufacturer's recommendations. The siRNA-mediated knockdown of *ESAM* was performed using a siGENOME SMARTpool specific for human *ESAM* (Dharmacon, Lafayette, CO). The confluent monolayer of HUVEC was transfected with the *ESAM* siRNA or Stealth RNAi negative control and using the Lipofectamine RNAiMAX reagent (Invitrogen).(Hara et al., 2009) After incubation for 24-48 hours, *in vitro* transmigration assays were performed using the *ESAM*-depleted HUVEC and THP-1 cells. In a subset of knockdown of adhesion molecules on macrophages, THP-1 cells were transfected with siRNA for *LFA-1, VLA-4, Mac1, JAM1, CD99,* or Stealth RNAi negative control (Thermo Fisher Scientific, Waltham, MA) for *in vitro* adhesion assays.

2.6 In vitro adhesion assay

The recombinant soluble form of ESAM was made as a fusion protein with the extracellular domain of ESAM and maltose-binding protein (MBP) and using the pMAL Protein Fusion and Purification System (New England Biolabs, Ipswich, MA). The cDNA for the extracellular domain of murine ESAM was obtained by PCR using the primers

5-tcagaattcatgattcttcaggctggaacccccgagacc-3' and

5-gactctagaggaccctgtcatcacgtccaaggtcacgtt-3', and cloned into the pMAL-C2X vector in the same translational reading frame as the *malE* gene encoding MBP. The fusion protein of the truncated ESAM and MBP (ESAM-MBP) was thus produced by using DH5α competent cells, and purified by means of amylose affinity chromatography according to the manufacturer's instruction. Adhesion assays using the truncated ESAM protein were performed as described previously.(Frankel et al., 1994) Briefly, culture dishes were coated with 2-10 μg of ESAM-MBP fusion protein or MBP (control). Monocyte/macrophage cell line THP-1, or J774.1 cells were labeled with 1 μmol/L calcein-AM (Molecular Probes, Eugene, OR), added onto the ESAM-MBP-coated dish, and incubated at 37 for 40 minutes. After washing 3 times, the number of adherent THP-1 cells or J774.1 cells was counted under a fluorescent microscopy.

2.7 *In vitro transmigration assay*

The *in vitro* transmigration assay was performed as described previously.(Faure et al., 2006; Liu et al., 2008) HUVEC or HAEC were grown to confluency in a 24-well culture insert (3-μm pore size Transwell; Corning, Tokyo, Japan) in 200 μL RPMI containing 10% fetal calf serum and 30 μg/mL endothelial cell growth supplements. After transfection of *ESAM* siRNA or non-target siRNA, 2.0×10^4 THP-1 cells in RPMI containing 0.2% fetal calf serum were added to the upper chamber. In the lower chamber, 500 μL RPMI containing 10 ng/mL monocyte chemoatrractant protein-1 (MCP-1, PeproTech, Rocky Hill, NJ) was placed to stimulate cell migration. Cells in the upper chamber were removed after 90 or 180 minutes, while transmigrated THP-1 cells in the lower chamber were labeled with calcein-AM and

counted under a fluorescent microscope.

2.8 Chemically induced peritonitis model

Thioglycollate-induced peritonitis was generated as described previously.(Bixel et al., 2007) Female *ESAM*-/- and *ESAM*+/+ mice, 10-14 weeks old, were used for this assay. Thioglycollate medium (4%) was injected into the peritoneal cavity to evoke macrophage-dominant inflammation. Four days later, the mice were sacrificed, and peritoneal lavage was performed with 10 mL of PBS. The total number of cells in the peritoneal fluid was determined with a cell counter.

2.9 Statistical analysis

Data were expressed as mean±SE. An unpaired Student *t* test was used to detect significant differences when two groups were compared. One-way ANOVA was used to compare the differences among three or four groups, followed by Bonferroni's test for post hoc analysis. *P* values less than 0.05 were considered statistically significant.

3. Results

3.1 Atherosclerosis is attenuated in mice with functional ESAM deletion

Male and female *apoE-/-* and *ESAM-/-apoE-/-* mice were evaluated for development of atherosclerosis. After 12 weeks on normal chow, when the mice were 16 weeks old, atherosclerotic lesion formation was evaluated by means of oil-red-O staining of sections at the aortic valve level (Fig. 1A). Extent of disease was quantified as total lesion area determined planimetrically. Interestingly, the atherosclerotic lesions were markedly attenuated in double

knockout mice compared with in *apoE-/-* mice: a significant decrease by 41% in males ($p<0.005$) and by 24% in females ($p<0.05$) (Fig. 1C). The aorta *en face* analysis by means of oil-red-O staining at the age of 16 weeks confirmed that plaque areas had decreased by 41% in *ESAM-/-apoE-/-* mice compared to in *apoE-/-* mice (Fig. 1B and 1D). Therefore, targeted inactivation of *ESAM* in *apoE-/-* mice results in a marked reduction of the size of the atherosclerotic lesion.

3.2 Plasma lipid profiles do not explain attenuated atherosclerosis in ESAM-/- mice

To investigate the mechanism by which atherosclerosis was attenuated in the double knockout animals, lipid profiles were obtained from control *ESAM+/+*, single knockout *apoE-/-*, *ESAM-/-*, and double knockout *ESAM-/-apoE-/-* male and female mice on normal chow diets. There were significant differences in lipid profiles among the mouse groups (Table 1). Male and female *ESAM-/-* mice showed modestly higher T-cho and triglyceride levels than *ESAM+/+* mice did, whereas HDL-C levels were not statistically different between the two groups. As for *apoE-/-* animals, male and female *ESAM-/-apoE-/-* mice showed markedly higher T-cho, HDL-C, and triglyceride levels than did *apoE-/-* mice. As a result, there were no significant differences in T-cho/HDL ratio between *ESAM-/-apoE-/-* and *apoE-/-* mice (Table 1). Thus, although ESAM deficiency resulted in an increase in plasma levels both of atherogenic and antiatherogenic lipoproteins in *apoE-/-* animals, the plasma lipid profiles did not explain the attenuated atherosclerosis in *ESAM-/-apoE-/-* mice.

3.3 ESAM expression in the vascular wall may correlate with plaque neovascularization

Since the lipoprotein profile in *ESAM-/-apoE-/-* animals did not provide a clear indication of

the mechanism for the decrease observed in atherosclerosis, we investigated differences in the vascular wall of the *apoE*-/- single and *ESAM-/-apoE-/-* double knockout mice. Because *ESAM* deficiency has been shown to reduce pathological angiogenesis in mice, we assessed neovascularization (vasa vasorum) around the atheroma in each section. The total number of blood vessels in the adventitia was less in *ESAM-/-* mice than in WT mice (Fig. 2A vs. 2D, and 2G). Similarly, the total number of blood vessels was less in *ESAM-/-apoE-/-* mice than in *apoE-/-* mice (Fig. 2B vs. 2E, and 2G). When we compared the number of vessels by size, small vessels in particular, those under 50 μm in diameter, were markedly reduced in *ESAM-/-apoE-/-* mice (Fig. 2H), supporting the notion of attenuated neovascularization resulting from *ESAM* deficiency. A whole-mount immunofluorescein study using fluorescein-conjugated isolectin revealed that formation of vasa vasorum in *ESAM-/-apoE-/-* mice was significantly attenuated compared with that in *apoE-/-* mice (Fig. 2C vs. 2F, and 2I). These findings indicate that *ESAM* deficiency results in a reduction in plaque angiogenesis around the atheroma.

3.4 ESAM regulates monocyte infiltration and complexity of atherosclerotic lesions

To further examine whether lesions in the *apoE-/-* and *ESAM-/-apoE-/-* mice had different cellular composition, we analyzed the atherosclerotic areas by histological and immunohistochemical stainings of with antibodies chosen to specifically label different cell types. Masson's Trichrome and Elastica van Gieson stainings revealed higher elastic fiber and lower collagen fiber contents in the plaque lesion in *ESAM-/-apoE-/-* than in *apoE*-/- mice (Fig. 3A). Next, an antibody to MOMA-2 was employed to evaluate the area containing infiltrating macrophages (Figs. 3A and 3B). The percentage of MOMA-2-stained areas in the

aortic sinus lesions was significantly smaller in *ESAM-/-apoE-/-* mice, which is consistent with the overall smaller number of macrophages in these lesions (Fig. 3B). There were no significant differences in the T-cell or smooth muscle cell compositions of the lesions in the *apoE-/-* and the *ESAM-/-apoE-/-* mice as demonstrated immunohistochemically with antibodies to CD3 or smooth muscle α-actin, respectively (*data not shown*). Therefore, ESAM deficiency appeared to reduce not only the size and macrophage content but also the complexity of the atherosclerotic lesions.

To clarify whether the reduced macrophage recruitment is reproducible, we used another model of the *in vivo* transmigration assay. Chemically induced peritonitis is a well-characterized model for macrophage recruitment in sites of acute inflammation *in vivo*. The assay using this model showed that the number of transmigrated macrophages in the peritoneal cavity was significantly lower in *ESAM*-/- than in *ESAM*+/+ mice (Fig. 3C), suggesting ESAM may contribute to the recruitment of macrophages while inflammatory cells go through the endothelial cells.

3.5 Knockdown of ESAM in endothelial cells reduced transmigration of monocytes

To investigate the mechanism underlying the reduced macrophage content by *ESAM* deficiency, the *in vitro* transmigration assay was performed using an *ESAM*-depleted endothelial monolayer and THP-1 cells. When *ESAM* was downregulated in the monolayer of HUVEC, the transmigration of THP-1 cells was significantly attenuated compared to control siRNA treatment with 90-minute incubation. However, when a longer incubation of over 180 minutes was used, there was no significant difference between the two groups (Fig. 4A). Similar results were obtained in case with HAEC (Fig. 4B). These findings indicate that

ESAM may regulate adhesion of macrophage to the endothelium and early-phase macrophage infiltration into the vascular tissue.

Furthermore, we documented a direct interaction between ESAM and THP-1 cells by means of the adhesion assay using truncated ESAM-MBP or MBP only (Fig. 5). As shown in Fig. 5B, coating of the culture plate with ESAM-MBP enhanced the adhesion of THP-1 in an ESAM dose-dependent manner compared to adhesion after the control MBP treatment. We confirmed similar results by adhesion assays using mouse monocyte/macrophage cell line J774.1 (*data not shown*). Thus, these findings support the notion of a measurable decrease in the macrophage composition of ESAM-negative lesions, and indicate a possible mechanism by which ESAM may have a direct impact on the development of vascular wall disease.

3.6 VLA-4, LFA-1, JAM1, MAC-1, or CD99 did not interact with ESAM

Because ESAM was not expressed by macrophages,(Hirata et al., 2001) we examined the validity of the hypothesis that a heterophilic ligand of ESAM is present on the macrophages, which regulates the interaction between monocytes and endothelial cells. Using siRNA techniques, we suppressed the expression of well-known adhesion receptors on macrophages, and followed this with *in vitro* adhesion assays. As shown in Fig. 6, downregulation of *VLA-4, LFA-1, JAM1, Mac1, or CD99* in THP-1 did not affect the adhesion of THP-1 cells to the ESAM-MBP-coated plates. This indicates that ESAM probably interacts with unidentified ligand(s) other than these molecules on THP-1 cells.

4. Discussion

The study presented here demonstrated that targeted inactivation of *ESAM* in *apoE*-/- mice

resulted in a robust decrease in the size and complexity of atherosclerotic lesions in the aorta. However, *ESAM*-/-*apoE*-/- mice showed higher plasma levels both of atherogenic and antiatherogenic lipoproteins than control *apoE*-/- mice, while the T-chol/HDL ratio was similar between *apoE*-/- and *ESAM*-/-*apoE*-/- mice. Although the reason for this difference in lipid profiles remains unclear, a plausible explanation for the lipid profile would be the delayed clearance of plasma lipoproteins as a result of *ESAM* deletion. ESAM is expressed in sinusoidal endothelial cells in the liver.(Jamieson et al., 2007) It has been reported that degeneration of sinusoidal fenestration under pathological conditions or with aging inhibits the uptake of lipoproteins by hepatocytes, which can be a cause of hyperlipidemia (DG et al., 2007; Khandoga et al., 2009). In this connection, we recently documented a significant role for ESAM in the maintenance of endothelial fenestration, in that *ESAM* deletion was found to reduce the fenestration of endothelial cells in the glomeruli.(Hara et al., 2009) We therefore speculate that *ESAM* deletion may retard the clearance of plasma atherogenic lipoproteins through causing disorganization of sinusoidal endothelial fenestration. Further studies are required, however, to elucidate the effect of *ESAM* deficiency on plasma lipid profile.

Although changes in plasma lipid profiles are not sufficient to explain the attenuation of atherosclerosis in *ESAM*-/-*apoE*-/- mice, we found that *ESAM* deletion markedly reduced the number and vasa vasorum in the adventitia. A number of studies have suggested that the development of vasa vasorum is associated with that of atherosclerotic lesions in humans and hypercholesterolemic animal models.(Langheinrich et al., 2006; Moulton et al., 2003; Virmani et al., 2000; Williams et al., 1988) We previously reported that targeted inactivation of *ESAM* attenuates tumor angiogenesis,(Ishida et al., 2003) which was primarily attributable to a reduction in endothelial migration and tube formation. It is therefore reasonable to speculate

that the impairment of new blood vessel formation in the adventitia resulted in the reduction of the atherosclerotic lesion size in *ESAM*-/- mice. We confirmed that expression of the most potent angiogenic factor VEGF and its receptor VEGF-R2 were not decreased by *ESAM* deficiency (*data not shown*). Thus, the loss of *ESAM* is likely to have directly inhibited angiogenesis in our mode. The impairment of plaque angiogenesis may then have prevented the vascular tissue both from absorbing the nutrient and oxygen supply and from inhibiting the access of inflammatory cells to the plaque.

ESAM has been shown to perform important functions in neutrophil transmigration, although the mechanisms of these functions are not yet fully understood. Wegmann and colleagues have demonstrated that ESAM is involved in the extravasation of leukocytes at an early stage of the inflammatory process, although ESAM does not bind to neutrophils directly.(Wegmann et al., 2006) In addition, they showed that a lack of *ESAM* upregulates the expression of vascular endothelial growth factor (VEGF) and increases endothelial permeability. Hara and colleagues have reported that the tight junction in *ESAM*-/- mice was morphologically wide and irregular compared to that in *ESAM*+/+ mice, which resulted in an increase in permeability.(Hara et al., 2009) It is therefore thought that these changes in endothelial permeability may affect the process of monocyte infiltration. On the other hand, our study has shown for the first time that monocyte/macrophage cell line THP-1 or J774.1 cells directly bind to recombinant the ESAM protein, possibly through interaction with putative heterophilic ligand(s) on the cell. Thus, it is likely that ESAM may be involved in the adhesion and transmigration of circulating monocytes within the vessel wall, and subsequently promote macrophage infiltration into the plaque. Protein-protein interactions between hematopoietic and endothelial cells have been shown to regulate leukocyte

recruitment in tissue. For example, integrin interactions with the immunoglobulin superfamily, which includes JAM-1 as a ligand of LFA-1, contribute to LFA-1 dependent transendothelial migration of T cells and neutrophils as well as LFA-1-mediated arrest of T cells.(Ostermann et al., 2002) In addition, Mac-1 with ICAM-1, VLA-4 with VCAM-1, and $\alpha_V ß_3$ with platelet-endothelial cell adhesion molecule all mediate the transmigration or adhesion of leukocytes.(Diamond et al., 1991; Elices et al., 1990; Piali et al., 1995) As far as we were able to investigate the functions of several candidates for adhesion receptors in our siRNA-mediated knockdown study, none of VLA-4, JAM-1, MAC-1, LFA-1, or CD99 appeared to be involved in the ESAM-monocyte interaction. Although no ESAM heterophilic ligand was identified in our study, further investigation is needed to determine whether ESAM can modulate monocyte adherence and transit into the vessel wall through an as yet unidentified counter receptor.

The role of ESAM in atherosclerosis in humans remains unclear. Recently, Rohatgi and colleagues measured plasma levels of soluble ESAM in human subjects in the Dallas Heart Study.(Rohatgi et al., 2009) They reported that soluble ESAM is associated with subclinical atherosclerosis, and that an increase in soluble ESAM levels was associated with major cardiovascular risk factors as well as with multiple inflammatory markers. In combination of our findings, regardless of whether or not it is secreted, expression of ESAM *in vivo* is likely to positively correlate with the progression of atherosclerosis. In this context, plasma levels of soluble ESAM may be in parallel with the full-length ESAM expression in endothelial cells. These findings suggest that ESAM may be a biomarker and modulator of atherosclerosis in humans as well. Detailed structure and function of soluble ESAM remain unclear, and further studies are required to establish the distinct role of soluble and full-length ESAM expression

on the genesis of atherosclerosis.

In summary, *ESAM* deficiency in *apoE*-/- mice, regardless of its plasma lipoprotein profile, reduces the size and complexity of atherosclerotic lesions through inhibition of vasa vasorum formation around the plaque, and through the loss of ESAM-mediated binding of monocytes with the vessel wall. Ours is the first evidence to suggest that ESAM acts as a ligand for an as yet unidentified counter receptor on monocytes/macrophages and promotes the extravasation of macrophages into the vessel wall. Our study thus provides a novel insight into the molecular genesis of atherosclerosis.

Funding Information

This research was supported by a Grant-In-Aid for Scientific Research, a Grant for the 21st Century COE Program from the Ministry of Education, Culture, Sports, Science and Technology of Japan; a Bayer Grant for Clinical Vascular Function from the Kimura Memorial Heart Foundation; and a grant from the Japan Foundation of Cardiovascular Research.

Acknowledgments

None.

Conflict of Interest: None declared.

Figure Legends

Figure 1. Characterization of atherosclerotic lesions in apoE-/- and ESAM-/-apoE-/- mice

(A) Representative photomicrographs of aortic root sections from *ESAM*+/+, *ESAM*-/-, *apoE*-/- and *ESAM*-/-*apoE*-/- mice fed on normal diet for 12 weeks. Stainings with hematoxylin and eosin (H&E) and Oil-red-O were shown. (B) Whole aortas were longitudinally opened and atherosclerotic lesions were stained with oil-red-O. (C) Total lesion area of five sections in the aortic root from each mouse was quantified morphometrically. The atherosclerotic lesion areas were significantly attenuated in *ESAM*-/-*apoE*-/- mice compared with in *apoE*-/- mice. **P*<0.05, and ***P*<0.05 vs. corresponding *apoE*-/- group (n = 12, male; n = 9, female). (D) Quantitative analysis of *en face* atherosclerotic aortas in 20-week-old male mice showed that the lesions were significantly more attenuated in *ESAM*-/-*apoE*-/- than in *apoE*-/- mice. Percentage of lesion area represents the lesion area compared with total aortic area. **P*<0.05 vs. *apoE*-/- group (n = 7).

Figure 2. ESAM deletion reduces the number of adventitial vessels

Sections of descending aortas from wild-type mice (A), *apoE*-/- (B, C), *ESAM*-/-mice (D), or *ESAM*-/-*apoE*-/- mice (E, F) were probed for isolectin (red) and α-SMA (green). The total number of adventitial vessels (*arrows*) was less in *ESAM*-/- (D) and *ESAM*-/-*apoE*-/- (E) than in wild-type mice (A) and *apoE*-/- mice (B), respectively; quantification shown in (G). In particular, the number of small vessels (<50 μm in diameter) in the adventitia was significantly less in *ESAM*-/-*apoE*-/- than in *apoE*-/- mice; quantification shown in (H). **P*<0.05 vs. *apoE*-/- group (n=8). Magnifications: x20. For whole mount analysis of vasa vasorum (C

and F), descending aortas were probed for isolectin. Confocal Z-stack images of adventitial vessels were reconstructed with the LSM Image Browser. The vessel area, shown in red and calculated with Image J software, was significantly reduced in *ESAM*-/-*apoE*-/- mice compared with that in *apoE*-/- mice (I). **P*<0.05 vs. *apoE*-/- group (n=5).

Figure 3. Macrophage content and complexity of the atherosclerotic lesions

(A) After the *apoE*-/- and *ESAM*-/-*apoE*-/-mice were fed with normal diet for 20 weeks, the aortic lesion was stained with Masson's Trichrome, Elastica van Gieson, or anti-macrophage MOMA-2 antibodies. (B) Representative images of the MOMA2-positive area were shown. The MOMA2-positive area in the lesions of these two groups was compared. The macrophage content in atherosclerotic lesions was less in *ESAM*-/-*apoE*-/- than in control *apoE*-/- mice. **P*<0.05 (n=10). (C) Macrophage recruitment was evaluated using a thioglycollate-induced peritonitis model. The number of migrated macrophages in the peritoneal lavage of *ESAM*-/- mice was less than that in *ESAM*+/+ mice (**P*<0.05, n=12).

Figure 4. Macrophage/monocyte transmigration in vitro

Effect of *ESAM*-knockdown in endothelial cells on transmigration of THP-1 cells. After confluent HUVEC (A) or HAEC (B) in a 24-well cell culture insert (3-μm pore size) was transfected with *ESAM* siRNA or non-targeting siRNA, THP-1 cells were added to the top chamber and stimulated with 10 ng/mL MCP-1. Western blotting confirmed the downregulation of *ESAM* in HUVEC and HAEC (left panels in A and B, respectively). After incubation for 90- or 180-minutes, the number of cells transmigrated into the lower chamber was counted . *ESAM*-knockdown was found to retard early transendothelial migration of

THP-1 cells. (right panels in A and B, respectively) *P<0.05 (n=12).

Figure 5. In vitro adhesion assay of THP-1 cells and ESAM-coated plates

(A) Polyacrylamide gel electrophoresis with Coomassie staining showing a maltose-binding protein (MBP, control) and a fusion protein with truncated ESAM and MBP (ESAM-MBP). (B) After the culture dishes were coated with 10 μg MBP, 2.0 μg or 10 μg ESAM-MBP, THP-1 cells were added to the plates and incubated at 37°C for 40 minutes. The number of adherent THP-1 cells was counted under a fluorescent microscope. The number of adherent THP-1 cells was higher on ESAM-MBP-coated than on control plates. *P<0.005, †P<0.0001 (n=8 per group). Representative images of the migration assay were shown (bottom panels).

Figure 6. In vitro adhesion assay using siRNA transfection

THP-1 cells were transfected with siRNA for *VLA-4, JAM-1, MAC-1, LFA-1, or CD99* (the expressions were shown in upper panel), and then added onto ESAM-MBP-coated plates. The number of adherent THP-1 cells was then counted and showed that knockdown of *VLA-4, JAM-1, MAC-1, LFA-1, or CD99* in THP-1 cells did not significantly affect adhesion to ESAM-MBP-coated plates.

References

Bixel, M. G., et al., 2007. A CD99-related antigen on endothelial cells mediates neutrophil but not lymphocyte extravasation in vivo. Blood. 109**,** 5327-36.

Bolla, M. K., et al., 1999. Rapid determination of apolipoprotein E genotype using a heteroduplex generator. J Lipid Res. 40**,** 2340-5.

Cybulsky, M. I., et al., 2001. A major role for VCAM-1, but not ICAM-1, in early atherosclerosis. J Clin Invest. 107**,** 1255-62.

DG, L. E. C., et al., 2007. Age-related changes in the liver sinusoidal endothelium: a mechanism for dyslipidemia. Ann N Y Acad Sci. 1114**,** 79-87.

Diamond, M. S., et al., 1991. Binding of the integrin Mac-1 (CD11b/CD18) to the third immunoglobulin-like domain of ICAM-1 (CD54) and its regulation by glycosylation. Cell. 65**,** 961-71.

Drinane, M., et al., 2009. The antiangiogenic activity of rPAI-1(23) inhibits vasa vasorum and growth of atherosclerotic plaque. Circ Res. 104**,** 337-45.

Elices, M. J., et al., 1990. VCAM-1 on activated endothelium interacts with the leukocyte integrin VLA-4 at a site distinct from the VLA-4/fibronectin binding site. Cell. 60**,** 577-84.

Faure, V., et al., 2006. The uremic solute p-cresol decreases leukocyte transendothelial migration in vitro. Int Immunol. 18**,** 1453-9.

Frankel, G., et al., 1994. Characterization of the C-terminal domains of intimin-like proteins of enteropathogenic and enterohemorrhagic Escherichia coli, Citrobacter freundii, and Hafnia alvei. Infect Immun. 62**,** 1835-42.

Hara, T., et al., 2009. Endothelial cell-selective adhesion molecule regulates albuminuria in diabetic nephropathy. Microvasc Res. 77**,** 348-55.

Hirata, K., et al., 2001. Cloning of an immunoglobulin family adhesion molecule selectively expressed by endothelial cells. J Biol Chem. 276**,** 16223-31.

Ishida, T., et al., 2003. Targeted disruption of endothelial cell-selective adhesion molecule inhibits angiogenic processes in vitro and in vivo. J Biol Chem. 278**,** 34598-604.

Jamieson, H. A., et al., 2007. Caloric restriction reduces age-related pseudocapillarization of the hepatic sinusoid. Exp Gerontol. 42**,** 374-8.

Khandoga, A., et al., 2009. Leukocyte transmigration in inflamed liver: A role for endothelial cell-selective adhesion molecule. J Hepatol. 50**,** 755-65.

Langheinrich, A. C., et al., 2006. Correlation of vasa vasorum neovascularization and plaque

progression in aortas of apolipoprotein E(-/-)/low-density lipoprotein(-/-) double knockout mice. Arterioscler Thromb Vasc Biol. 26, 347-52.

Ley, K., et al., 2007. Getting to the site of inflammation: the leukocyte adhesion cascade updated. Nat Rev Immunol. 7, 678-89.

Liu, D. Q., et al., 2008. Signal regulatory protein alpha negatively regulates beta2 integrin-mediated monocyte adhesion, transendothelial migration and phagocytosis. PLoS One. 3, e3291.

Moulton, K. S., et al., 2003. Inhibition of plaque neovascularization reduces macrophage accumulation and progression of advanced atherosclerosis. Proc Natl Acad Sci U S A. 100, 4736-41.

Nasdala, I., et al., 2002. A transmembrane tight junction protein selectively expressed on endothelial cells and platelets. J Biol Chem. 277, 16294-303.

Ostermann, G., et al., 2002. JAM-1 is a ligand of the beta(2) integrin LFA-1 involved in transendothelial migration of leukocytes. Nat Immunol. 3, 151-8.

Ozaki, M., et al., 2002. Overexpression of endothelial nitric oxide synthase accelerates atherosclerotic lesion formation in apoE-deficient mice. J Clin Invest. 110, 331-40.

Pan, J. H., et al., 2004. Macrophage migration inhibitory factor deficiency impairs atherosclerosis in low-density lipoprotein receptor-deficient mice. Circulation. 109, 3149-53.

Piali, L., et al., 1995. CD31/PECAM-1 is a ligand for alpha v beta 3 integrin involved in adhesion of leukocytes to endothelium. J Cell Biol. 130, 451-60.

Price, D. T., Loscalzo, J., 1999. Cellular adhesion molecules and atherogenesis. Am J Med. 107, 85-97.

Ritman, E. L., Lerman, A., 2007. The dynamic vasa vasorum. Cardiovasc Res. 75, 649-58.

Rohatgi, A., et al., 2009. Differential associations between soluble cellular adhesion molecules and atherosclerosis in the Dallas Heart Study: a distinct role for soluble endothelial cell-selective adhesion molecule. Arterioscler Thromb Vasc Biol. 29, 1684-90.

Ross, R., 1999. Atherosclerosis--an inflammatory disease. N Engl J Med. 340, 115-26.

Sprague, A. H., Khalil, R. A., 2009. Inflammatory cytokines in vascular dysfunction and vascular disease. Biochem Pharmacol. 78, 539-52.

Springer, T. A., 1990. Adhesion receptors of the immune system. Nature. 346, 425-34.

Sun, L., et al., 2009. RAGE mediates oxidized LDL-induced pro-inflammatory effects and atherosclerosis in non-diabetic LDL receptor-deficient mice. Cardiovasc Res. 82, 371-81.

Taddei, S., et al., 2003. Mechanisms of endothelial dysfunction: clinical significance and preventive non-pharmacological therapeutic strategies. Curr Pharm Des. 9**,** 2385-402.

Virmani, R., et al., 2000. Lessons from sudden coronary death: a comprehensive morphological classification scheme for atherosclerotic lesions. Arterioscler Thromb Vasc Biol. 20**,** 1262-75.

Wegmann, F., et al., 2006. ESAM supports neutrophil extravasation, activation of Rho, and VEGF-induced vascular permeability. J Exp Med. 203**,** 1671-7.

Williams, J. K., et al., 1988. Vasa vasorum in atherosclerotic coronary arteries: responses to vasoactive stimuli and regression of atherosclerosis. Circ Res. 62**,** 515-23.

Figure 1

Click here to download high resolution image

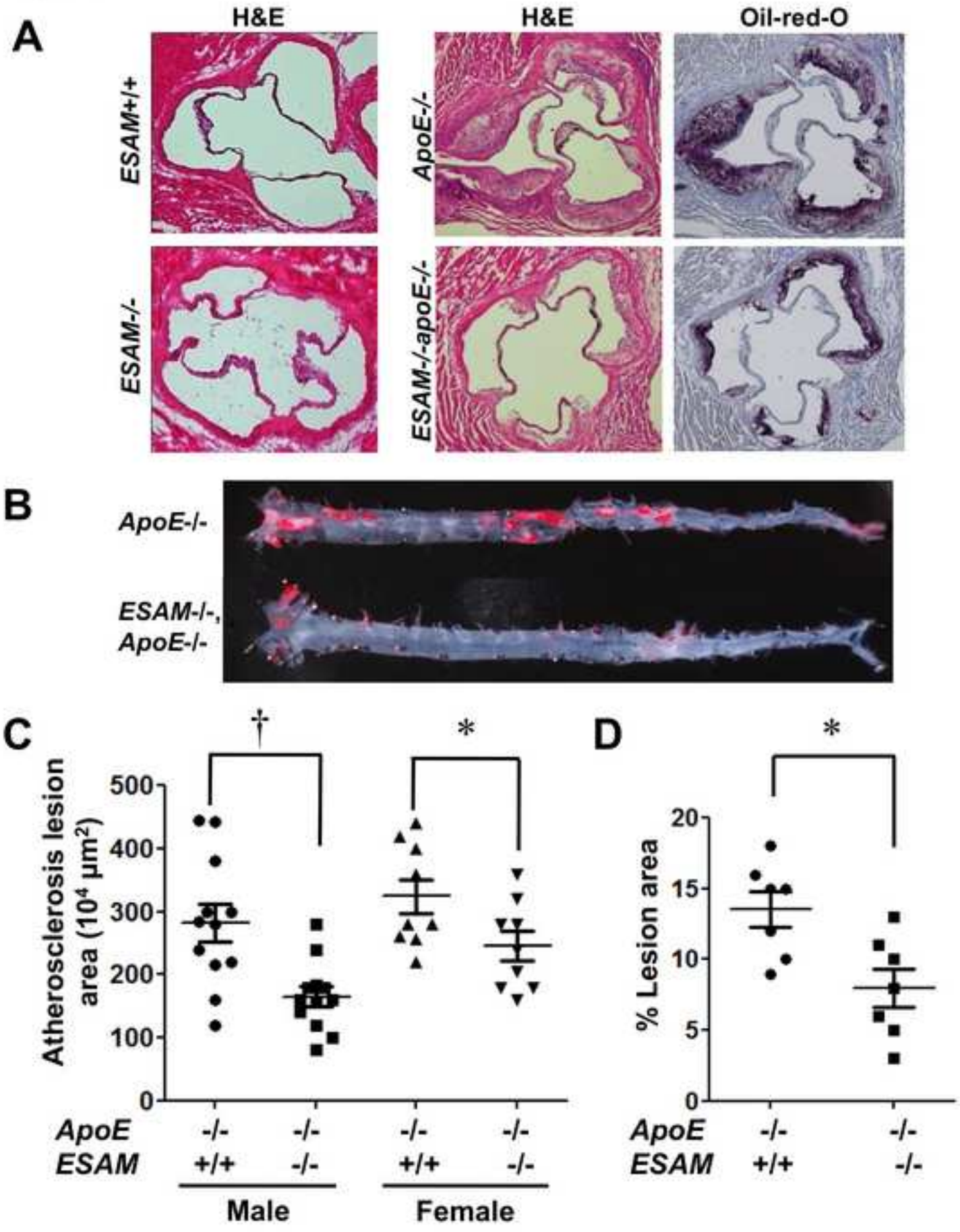

Figure 2

Click here to download high resolution image

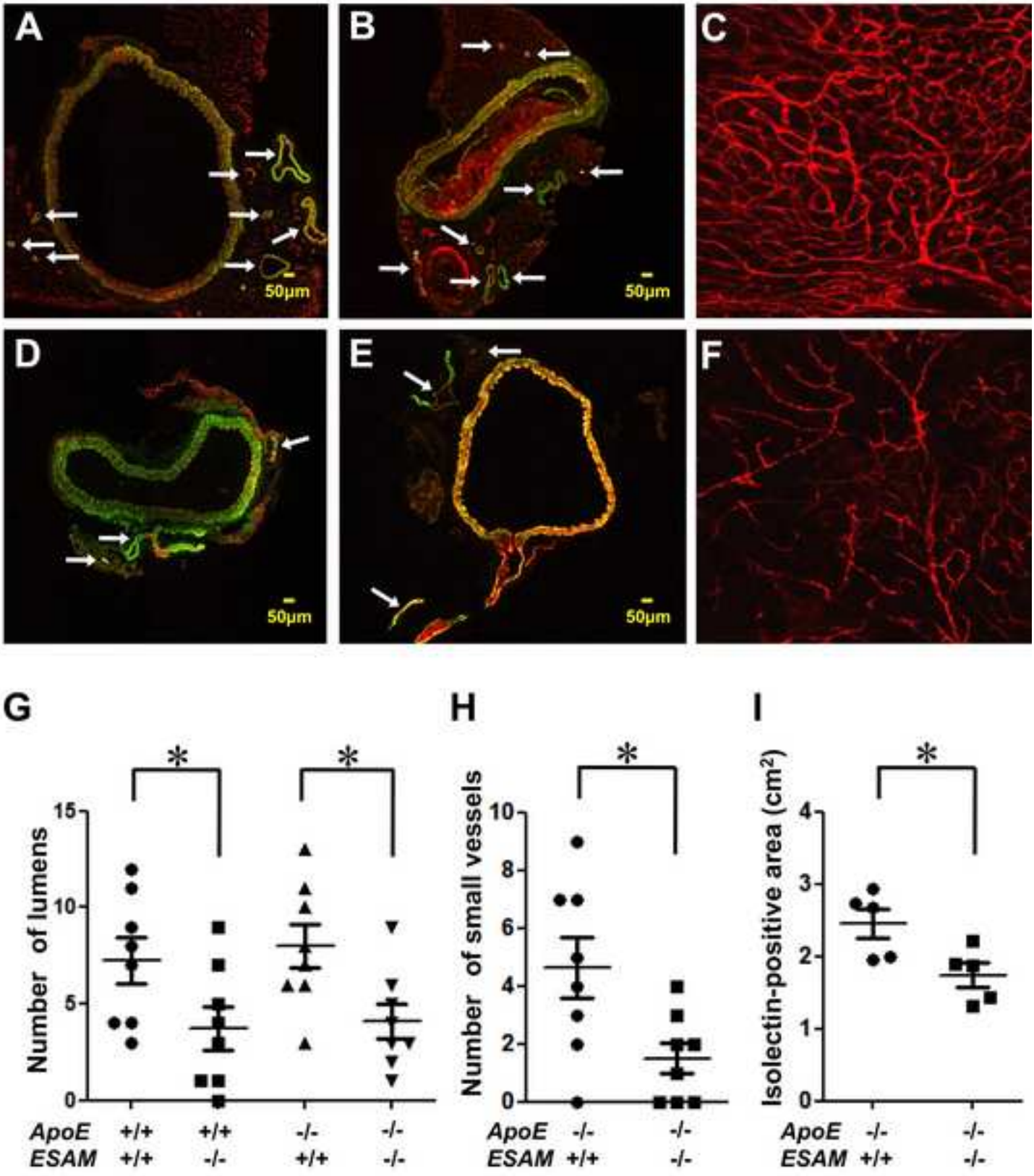

Figure 3

Click here to download high resolution image

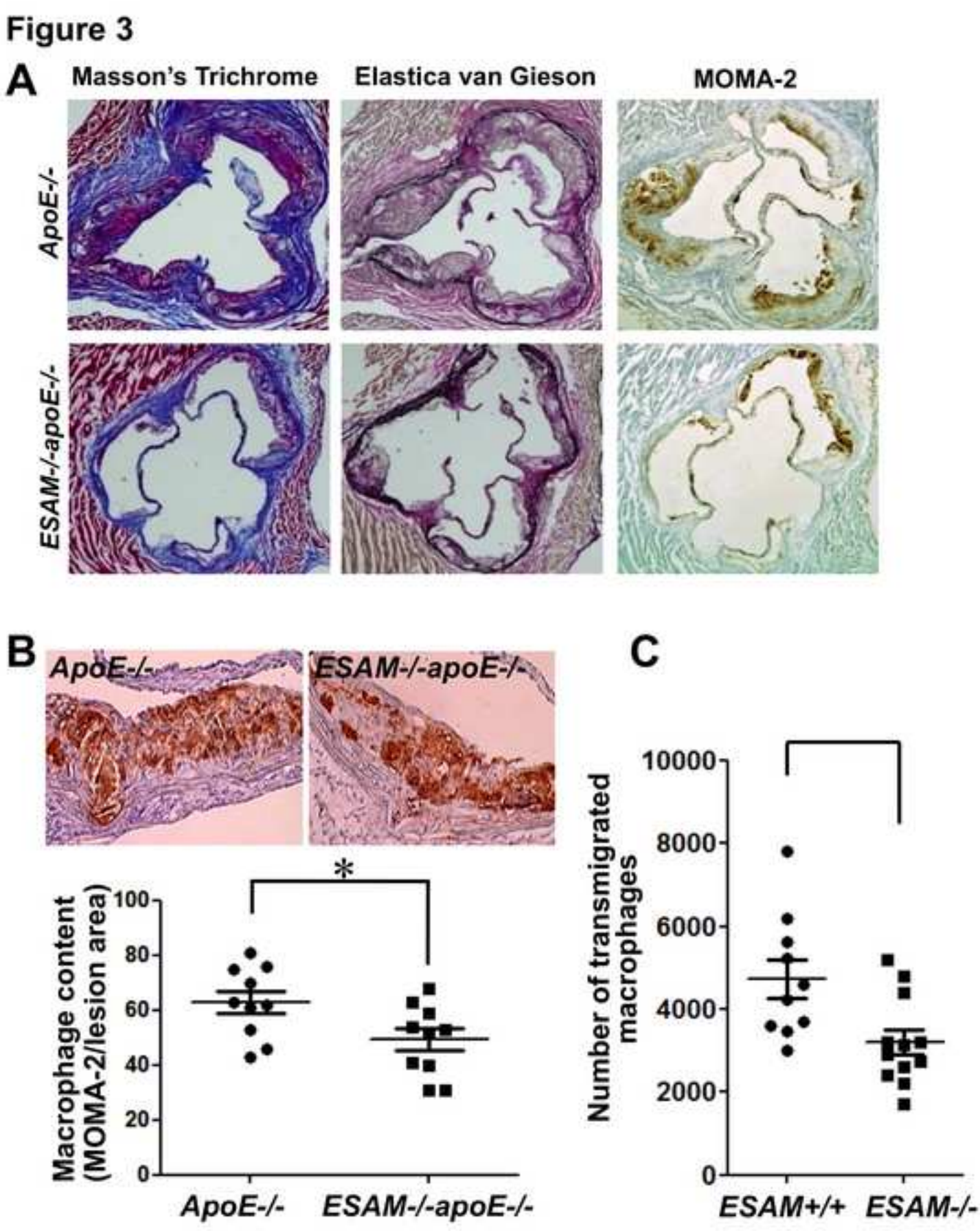

Figure 4

Click here to download high resolution image

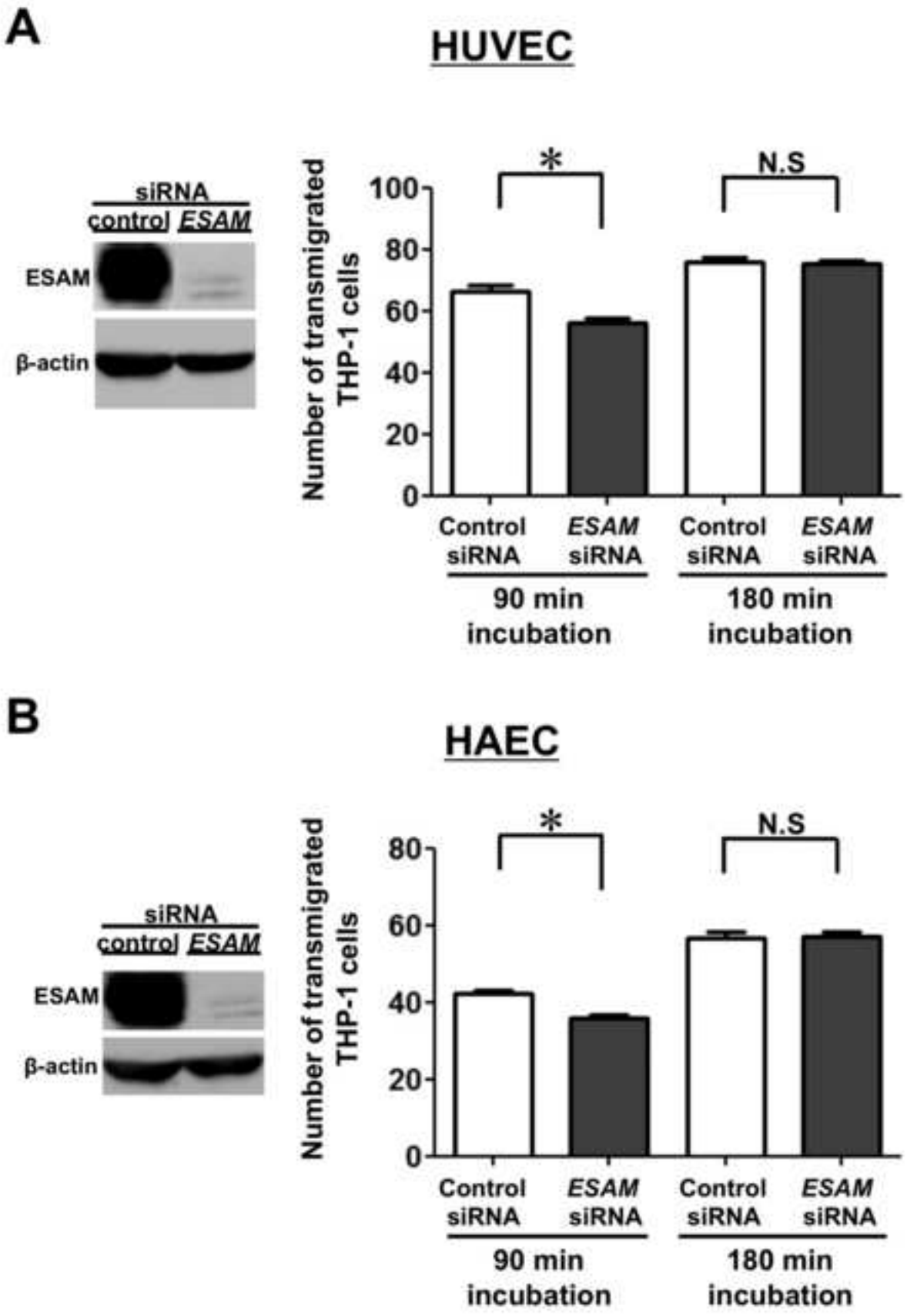

Figure 5

Click here to download high resolution image

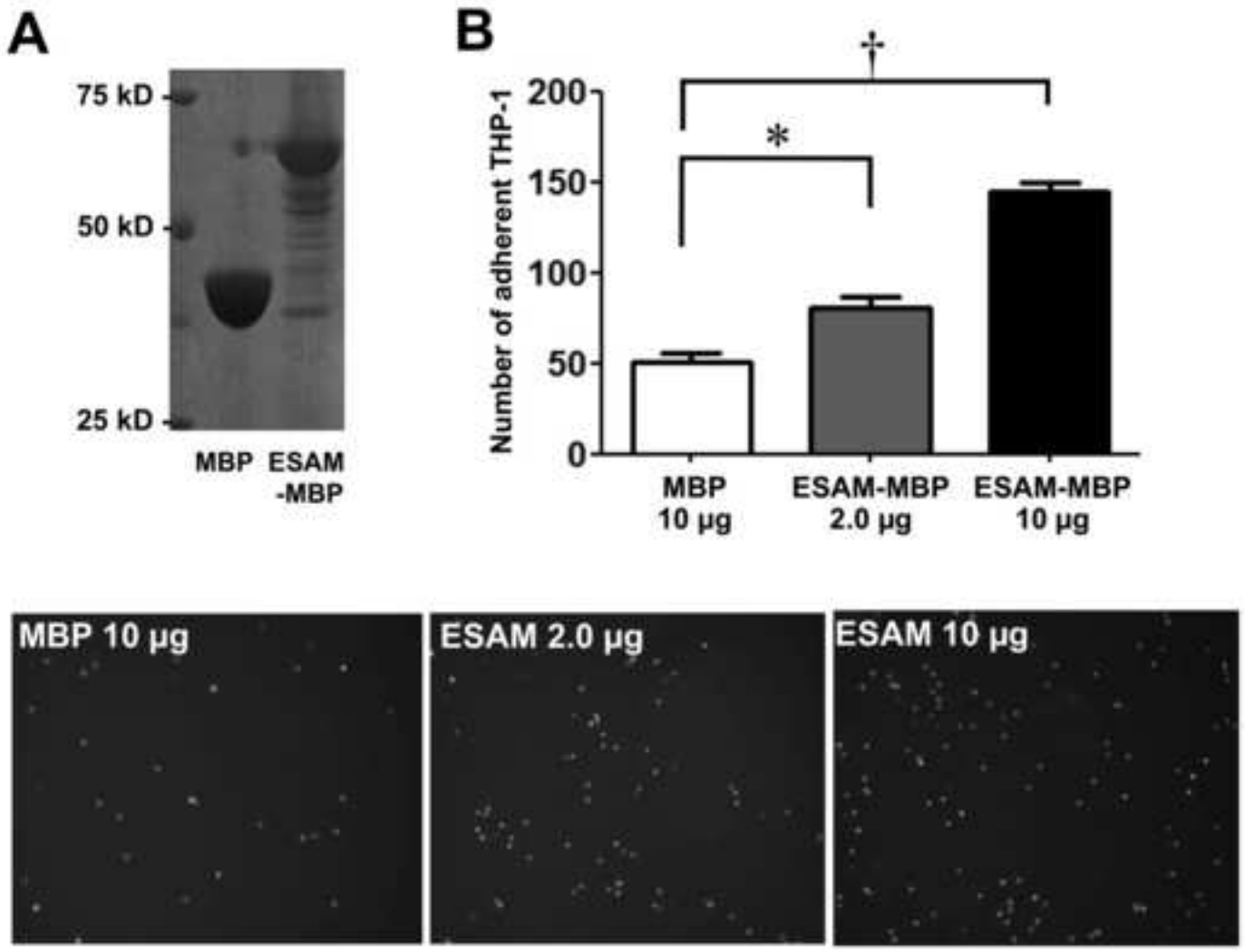

Figure 6

Click here to download high resolution image

Figure 6

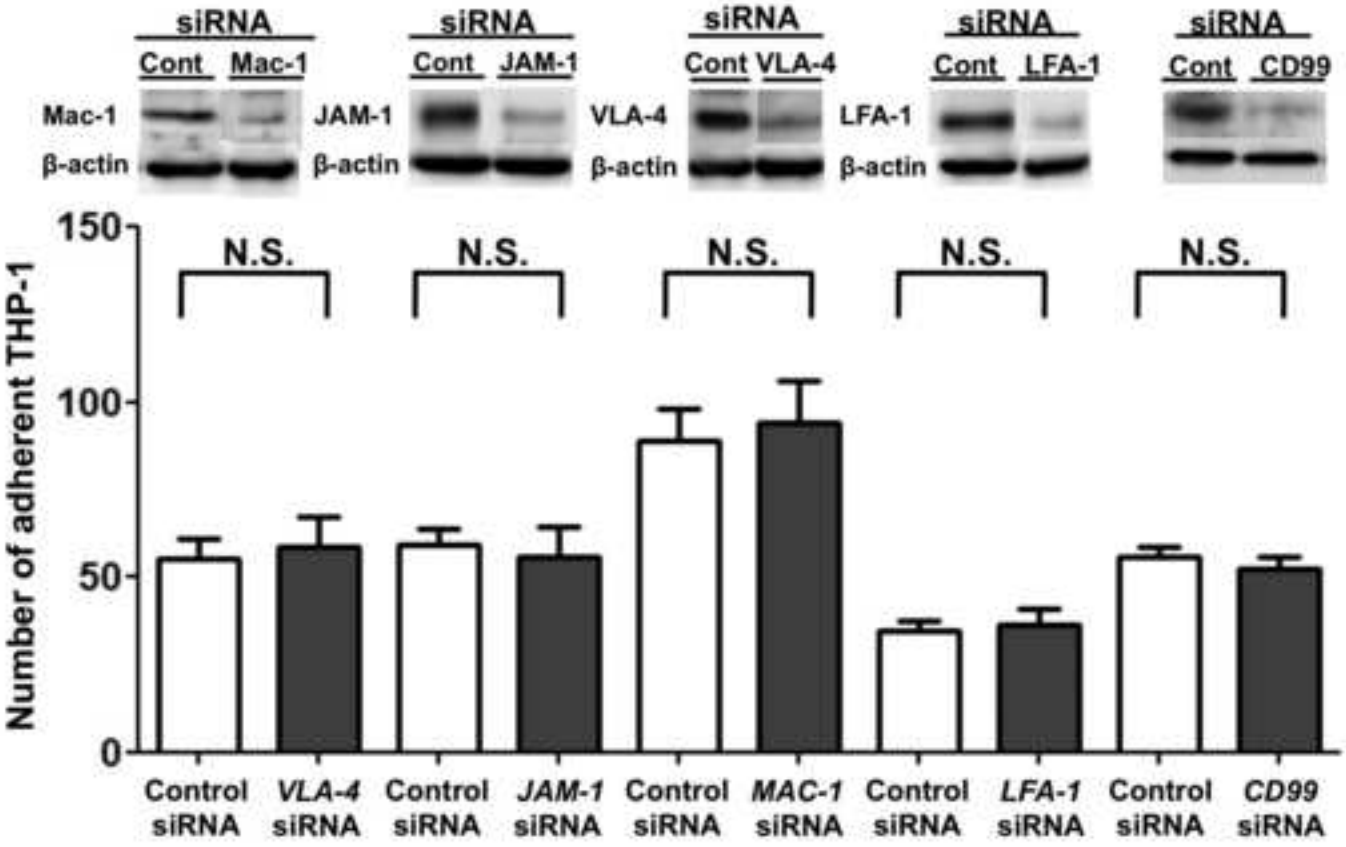

	ESAM+/+	*ESAM*-/-	*ESAM*+/+*apoE*-/-	*ESAM*-/-*apoE*-/-
Male mice				
T-cho	80.7±3.0	92.1±2.8*	582.8±24.4	806.2±41.1†
HDL-C	46.3±1.1	50.1±2.1	14.0±1.8	22.8±2.5†
Triglycerides	42.9±5.4	90.6±17.0*	68.1±10.5	113.9±15.1†
Female mice				
T-cho	65.7±1.9	75.0±5.3*	473.3±22.7	714.2±49.2†
HDL-C	37.8±1.7	38.7±3.6	8.3±0.8	21.2±3.8†
Triglycerides	27.9±8.1	51.0±5.7*	56.8±13.4	133.8±31.3†

Table 1. Fasting plasma lipid and lipoprotein profile

The plasma level of total cholesterol (T-cho), high-density lipoprotein cholesterol (HDL-C), and triglycerides was determined by biochemical assays. Values are expressed as mean±SE (mg/dL, n=10-12 in each group). *P<0.05 vs. *ESAM*+/+ mice, and †P<0.05 vs. *ESAM*+/+*apoE*-/- mice.